Optical Engineering

OpticalEngineering.SPIEDigitalLibrary.org

Interferometric system based on swept source-optical coherence tomography scheme applied to the measurement of distances of industrial interest

Eneas N. Morel
Nélida A. Russo
Jorge R. Torga
Ricardo Duchowicz

SPIE.

Interferometric system based on swept source-optical coherence tomography scheme applied to the measurement of distances of industrial interest

Eneas N. Morel,[a,*] Nélida A. Russo,[b] Jorge R. Torga,[a] and Ricardo Duchowicz[b,c]
[a]Universidad Tecnológica Nacional, Laboratorio de Optoelectrónica y Metrología Aplicada, Facultad Regional Delta, San Martin 1771, 2804 Campana, Buenos Aires, Argentina
[b]Centro de Investigaciones Ópticas (CONICET-CIC), Centenario y 506, 1897 Gonnet, La Plata, Buenos Aires, Argentina
[c]Universidad Nacional de la Plata, Facultad de Ingeniería, Calle 1 y 47, 1900 La Plata, Buenos Aires, Argentina

Abstract. We used an interferometric technique based on typical optical coherence tomography (OCT) schemes for measuring distances of industrial interest. The system employed as a light source a tunable erbium-doped fiber laser of ~20-pm bandwidth with a tuning range between 1520 and 1570 nm. It has a sufficiently long coherence length to enable long depth range imaging. A set of fiber Bragg gratings was used as a self-calibration method, which has the advantage of being a passive system that requires no additional electronic devices. The proposed configuration and the coherence length of the laser enlarge the range of maximum distances that can be measured with the common OCT configuration, maintaining a good axial resolution. A measuring range slightly >17 cm was determined. The system performance was evaluated by studying the repeatability and axial resolution of the results when the same optical path difference was measured. Additionally, the thickness of a semitransparent medium was also measured. [DOI: 10.1117/1.OE.55.1.014105]

Keywords: optical coherence tomography; metrological instrumentation; distance measurement.

Paper 151372 received Sep. 30, 2015; accepted for publication Dec. 11, 2015; published online Jan. 20, 2016.

1 Introduction

The current trend in the development of low-coherence interferometry or more widely known as optical coherence tomography (OCT)[1] shows significant growth in applications to the area of medicine, especially ophthalmology[2–4] and cardiology,[5,6] where commercial equipment has already been developed. On the other hand, the number of industrial and material applications of OCT has a slower growth that has been increasing in the last years. Currently most works are related to studies of surfaces, determination of refractive index, and studies of multilayer films where the depth measurement does not exceed 1 cm.[1] In our view, one of the industrial applications which has so far shown few results is in measuring distances longer than a centimeter. The use of OCT in this regime requires some versatility in the experimental setup. Three established techniques have the potential to meet this requirement: optical coherence tomography in the time domain-OCT (TD-OCT), spectral or Fourier domain-OCT (FD-OCT), and swept source-OCT (SS-OCT), each one with its particular limitations.

When using TD-OCT, the interference signal is generated from the displacement of a mirror in the reference arm of the interferometer[1–4] to equalize the sample distances. This involves the use of moving mechanical systems with high accuracy and resolution. Furthermore, for measuring longer distances, it should have an appropriate reference arm length, generating greater complexity in the system alignment, and in the demands of the positioning control system. Also this requirement is a strong limitation for the scanning frequency on the sample.

Moreover, FD-OCT allows the design of an interferometric system more robust than that of TD-OCT by not requiring the movement of the reference mirror,[6,7] thereby increasing the mechanical stability and reducing the sensitivity to vibrations. Here, a spectrometer is used to detect the interference signal, resulting in a smaller measuring range limited by the spectral resolution of the spectrometer. This constraint adds a second one, due to the presence of aliasing in the Fourier transform of the interference signal, which can cause a misinterpretation of measurements. For these reasons, the maximum imaging depth is typically <1 cm.

The SS-OCT technique offers an interesting alternative provided by the use of tunable light sources[8–13] such as optical fiber lasers with tunable Fabry–Perot (FP) filter or electro-optical modulators[9,] or recent systems based on semiconductor lasers like the MEMS-tunable vertical cavity surface emitting lasers,[11] and the Vernier-tuned distributed Bragg reflector laser.[12] In general, in these systems, it is possible to achieve a laser linewidth narrower than the resolutions typically obtained by a spectrometer. Consequently, the depth range, in this case given by the instantaneous linewidth of the laser (coherence length), can reach values in the order of a centimeter and greatly expand the potential industrial applications.[14–18] In this case, the detection system is a photodetector in conjunction with a digitizer or oscilloscope, simplifying the system.

Obviously, besides the narrow bandwidth emission, it is desirable that the optical source has a fast tuning over a large

*Address all correspondence to: Eneas N. Morel, E-mail: nmorel@frd.urn.edu.ar

0091-3286/2016/$25.00 © 2016 SPIE

wavelength range. How quickly this is possible is determined by the sweep speed of the optical filtering device which selects the laser's operating wavelength and the dynamical processes inside the laser cavity.

In general, scanning sources have the inherent problem of not being able to provide accurate information about the correspondence between the wavelength, the signal voltage applied to the tuning device, and the temporary location within each sweep.[19]

Some current works,[20,21] use a Mach–Zehnder interferometer with a balanced detector for detecting the spatial frequency, which is a relatively complex and dynamic system.

In this work, we propose a system based on SS-OCT for measuring large distances (capable of axial scanning up to 18 cm). A tunable fiber laser with emission in the spectral region near 1550 nm is used as light source and it has a sufficiently long coherence length to enable long depth range imaging. The design also includes a self-calibration arrangement implemented with a set of fiber Bragg gratings (FBGs)[22,23] used to pickoff specific wave numbers. In this way, it is possible to obtain a relationship between the spatial frequency (k) and the time (t), overcoming the aforementioned drawback. In addition, it has the advantage of being a passive system, which does not require additional electronic devices.

In the past, FBGs have been used to carry out the calibration procedure of the spectrometer used in an SD-OCT system.[24] In our case, the array of FBGs constitutes the stage of on-line calibration of an SS-OCT-based system.

2 System Overview

The measurement system comprises the stages shown in Fig. 1.

2.1 *Light Source*

An all-fiber tunable erbium ring laser operating in the range of 1520 to 1570 nm is used as the light source.[24–29] The ring configuration employs a fiber FP tunable filter (Micron Optics, FFP-TF2) with a free spectral range (FSR) of 60 nm and a bandwidth of 60 pm. The erbium-doped fiber is pumped through a wavelength division multiplexer, by a semiconductor laser diode emitting at 980 nm with maximum optical power of 145 mW. The fiber laser output beam is extracted from the ring cavity through the 10% port of a 10/90 optical coupler. The length of the doped fiber is selected taking into account a trade-off between spectral emission flatness and output power.

Applying a periodical signal like a triangular voltage waveform to the filter PZT actuator, the resonance wavelength of the FP cavity is adjusted and a laser sweep source is obtained. In our experimental setup, this was accomplished by using a fiber Fabry–Perot controller (FFP-C) from Micron Optics. The scanning frequency can be varied up to 100 Hz.

Figure 2 shows a laser scan captured with an optical spectrum analyzer (OSA) (Yokogawa, model AQ6370B) synchronized to the FP filter sweep. As it can be seen, the laser has a power emission fairly constant within the tuning range.

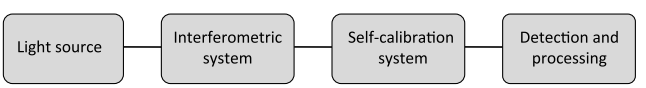

Fig. 1 Block diagram of the implemented system.

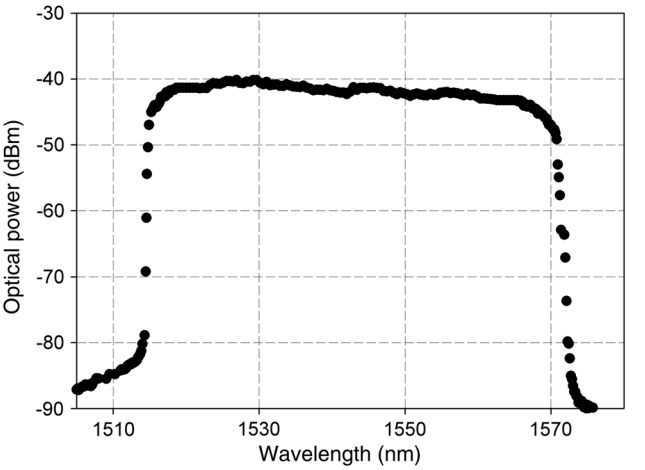

Fig. 2 Spectral response of the laser swept source.

Considering the rectangular spectral profile of the laser source when it sweeps a bandwidth of 60 nm, it is possible to achieve a theoretical maximum axial resolution of about 40 μm.

However, depending on the requirements it is possible to modify the spectral width of scanning by varying the control signal of the FP filter, which obviously worsens the axial resolution.

When the laser operates at any fixed wavelength within the tuning range, the emission spectrum has a typical width of 20 pm at 3 dB.

2.2 *Interferometric System*

The interferometric system consists of a Michelson interferometer and a nonmonochromatic light source with spectrum intensity

$$I_{r/s}(k) = I_{or/s} \cdot S\left(\frac{k-k_0}{\Delta k}\right), \tag{1}$$

where $S(k)$ represents the spectral shape of the light source, I_r and I_s are the reference and sample arm intensities, k and $k_0 = 2\pi/\lambda_0$ are the wave number and the central wave number of the source spectrum and Δk is its spectral width. By defining $\beta^2 = I_s/I_r$ as the visibility or modulation depth, the total intensity can be expressed as

$$I(k)_r S\left(\frac{k-k_0}{\Delta k}\right)[1+\beta^2+2\beta\cos(n_g \Delta z k)], \tag{2}$$

where $n_g \Delta z$ is the optical path difference (OPD), with n_g the group refraction index of the medium and Δz is the distance between both interferometer arms.[1,18–20]

The depth of measurement Δz_{MAX} is determined by Eq. (3), where δ_λ is the resolution of the detection system[18–20]

$$\Delta z_{MAX} = \frac{\lambda_0^2}{4 n_g \delta_\lambda}, \qquad \delta_\lambda = \frac{\Delta\lambda}{N_s}. \tag{3}$$

In these expressions, $\Delta\lambda$ is the spectral width of the light source and N_s is the number of samples.

2.3 *Self-Calibration System*

In applications of low-coherence interferometry by swept source, it is critical the linear sampling process of the spatial frequency (k-space). In the system used in this work, the laser-tuning process was performed by controlling the cavity of the FP filter. This process could be affected by various factors such as the hysteresis of the piezoelectric actuator (PZT) and errors in the control of repetition of the cycle of sweeping. This may lead to changes in the position of the PZT in each cycle and makes unknown the variation of k with time [$k(t)$]. Therefore, a suitable calibration method has to be used to compensate the errors.

The proposed self-calibration system consists of an array of FBGs centered at different wavelengths covering the spectrum emission of the optical source. Since the spectral locations of the filters are known, from the measurement of their temporal positions, it is possible to calibrate the OCT measurement system, resizing the time axis for each scan of the swept source.

The calibration process has a dual purpose:

a. To produce the linearization of the spectral interference signal in k-space by using the relationship between the measured time for each filter (t_{FBGi}) and the corresponding wave number (k_{FBGi}). This process allows obtaining an equally spaced scale in the k-space and eliminates variations in instantaneous frequency due to the dynamics of the PZT used to tune the light source.

b. To obtain the sampling frequency used in the calculation of the Fourier transform

$$f_s = \frac{1}{(k_{n-1} - k_n)}. \tag{4}$$

As it is well-known, FBGs are sensitive to thermal changes, so variations in the room temperature induce changes in their spectral positions. However, since all gratings that are part of the calibration system are recorded on the same type of optical fiber and all of them experience the same temperature change, this will not generate measurement errors in the proposed OCT scheme. This is because for measuring the displacement, only the value of the sampling frequency is needed. In that case, it is only relevant that the Δk value between gratings should be kept constant, even though their individual positions (k_i) could change. The change in the absolute spectral positions of the Bragg gratings due to thermal variations only generates a shift in the k-space and does not affect the determination of the sampling frequency.

Figure 3 shows the behavior of the fiber gratings used in the calibration system when a change of 5.3°C in the room temperature occurs. It is observed that all the gratings experience the same spectral shift of about 50 pm, compatible with the temperature sensitivity of such a component (~9.4 pm/°C).

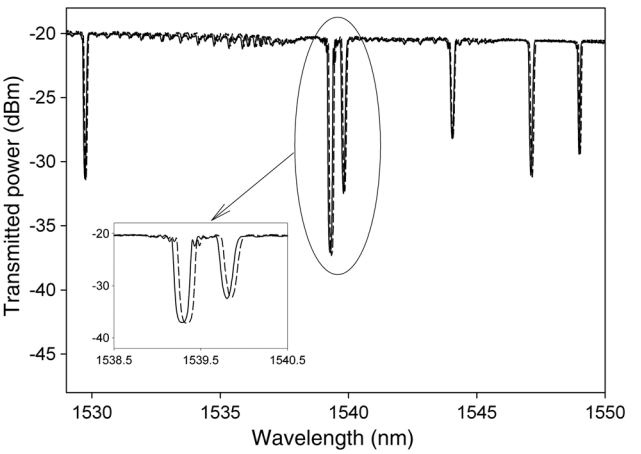

Fig. 3 Spectral shift of the FBGs due to a change in temperature of 5.3°C.

The number of fiber gratings to use is a trade-off between getting the best calibration curve to minimize the adjustment errors, and generate as little impairment as possible in the detected signal due to insertion losses and noise caused by back-reflections. The aim is to use a set of FBGs as a kind of "marks" that relate the spatial frequency and the time, but they need not be equally spaced.

2.4 *Detection and Processing*

The temporal distribution of the interference signals was obtained by using the internal photodetector of the fiber FP controller, which was connected to a digital oscilloscope. The acquired signals were subsequently processed as follows. At first, a high-pass filter was used to remove the DC component of the interference signal. By employing the Hilbert transform,[30,31] the envelope used for normalization was obtained. The chirp Fourier transform[32,33] was then applied allowing selecting a given bandwidth. In this way, the position of the interference peaks indicating the OPD between the interferometer arms was obtained.

3 System Characterization

The system was evaluated by studying the repeatability in the measurement of the same OPD. For this purpose, the experimental configuration of Fig. 4 was used.

In this case, the self-calibration system was composed of six Bragg gratings, centered on the following wavelengths: 1548.991 nm (FBG1), 1547.1285 nm (FBG2), 1544.056 nm (FBG3), 1539.819 nm (FBG4), 1539.305 nm (FBG5), and 1529.744 nm (FBG6), with a spectral width of the order of 0.1 nm.

In order to evaluate the repeatability of the results obtained, the laser source was continuously scanned and several records of the intensity detected in the same conditions were carried out.

To show the spectral position of the gratings, one arm of the interferometer was blocked to remove the interference modulation.

Signals corresponding to two of these measurements are shown in Fig. 5, where it is observed the attenuation peaks in the Bragg wavelengths of the different gratings as a function of time. The error in the determination of the temporal

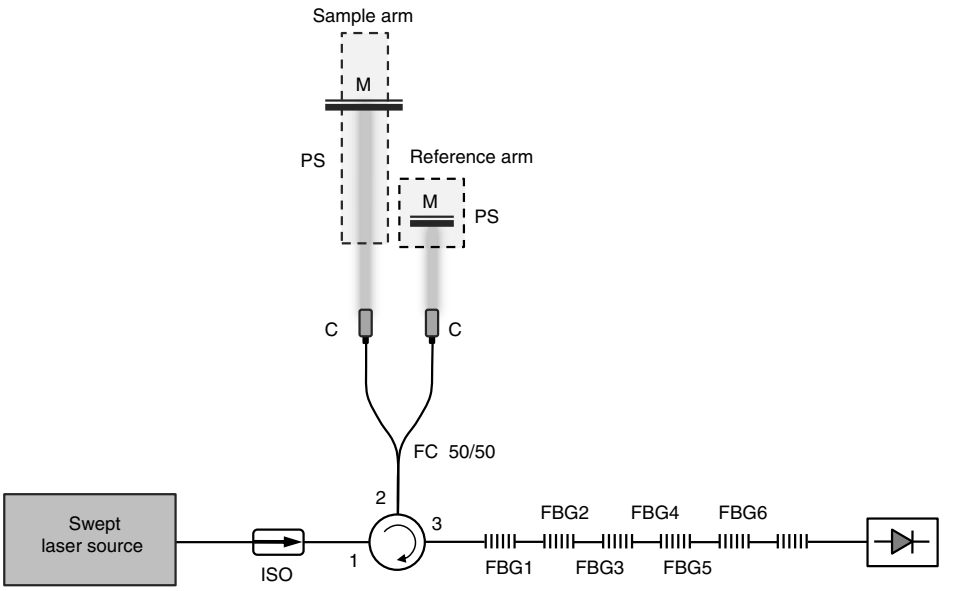

Fig. 4 Experimental scheme for system characterization (ISO, optical isolator; FC, fiber coupler; C, collimator; M, mirror; PS, positioning system; and FBG, fiber Bragg grating).

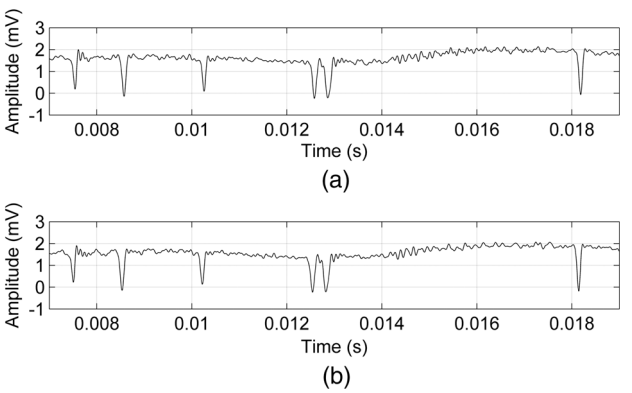

Fig. 5 (a) Signal detected and (b) Signal detected in different moments, avoiding reflections in the interferometer arms.

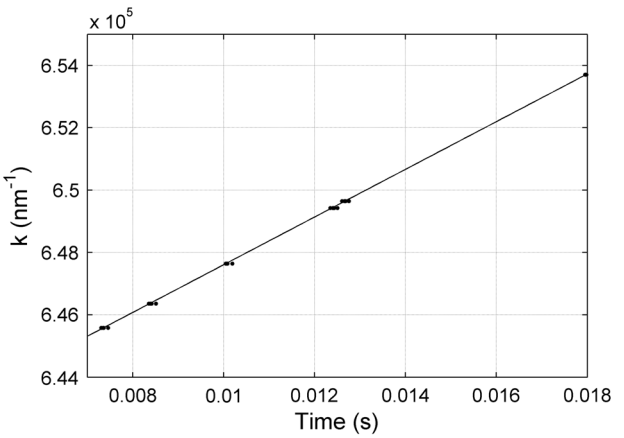

Fig. 6 Fitted curve k versus time.

position of each FBG is directly related with the shape and width of the peak profile, which in terms of time was in the order of 90 μs, when a sampling interval of 0.1 μs was used.

Then, for each measurement performed, the temporal positions were associated to the k value of each grating and a $k(t)$ relation was obtained after a fitting process, as explained in Sec. 2.3. In the example shown in Fig. 5, the best fit obtained is a linear curve.

The final calibration curve was obtained from an average of measurements identical to those of Fig. 5. In this case, a linear relation was obtained with an average slope value of 764.1×10^3 ms^{-1} and a dispersion of 1.3×10^3 ms^{-1} whereby a 0.17% percentage error arose, with the correlation factor between data and the interpolated curve of 0.99. In Fig. 6, it can be seen the different experimental points and the fit curve obtained using the average slope. The sampling frequency was determined from the slope of the fitted curves and results in these measurements $f_s = 6543$ m with a dispersion of 11.45 mm.

Thereafter, reflection from the interferometer arms was allowed and several measurements of the same OPD were made for the purpose of valuing the errors. A typical recorded signal is shown in Fig. 7.

Furthermore, in order to test different operating conditions of the system, a laser scanning of only 40 nm was used, which was selected to include the spectral region where the FBGs were located. Using the processing described above, the interference peak position for each signal was calculated, and then the mean value and standard

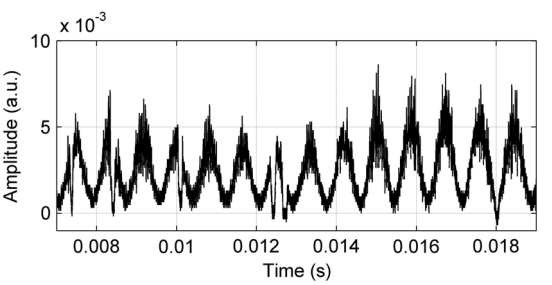

Fig. 7 Interference signal showing the positions of the FBGs for self-calibration.

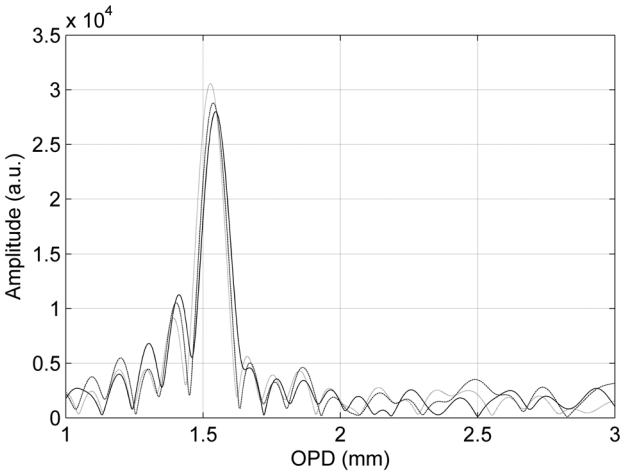

Fig. 8 Fourier transform of the interference signal.

deviation were obtained. In tests performed, 20 measurements of the same OPD were processed, although Fig. 8 only shows some of them for reasons of clarity. On average, the peak position was 1.556 mm with a deviation of 8 μm, corresponding to a percentage error in the measurement of 0.54%.

It is commonly accepted that the axial resolution in the OPD measurement is given by the FWHM of the peak of the Fourier transform of the interference signal. In this case, since we worked with a tuning range lower than the maximum possible using the bandwidth between FBG_1 and FBG_6 (around to 20 nm), the axial resolution worsened to ~80 μm. However, in our experiments, the statistical dispersion generally obtained in the measurement of the same distance was in the order of 10 μm.

4 Experimental Results

In order to test the proposed system, initially the configuration described below was used to measure the thickness of a semitransparent medium. Subsequently, a Michelson type setup was implemented to determine the maximum achievable measurement range.

4.1 *Thickness Measurement of Semitransparent Media*

In the first experiment, the system was tested measuring the thickness of a BK-7 glass plate of 1 ± 0.1 mm thick (WBK-251-1 model, UQG-Optics) using the setup shown in Fig. 9.

The sample (Sa) was illuminated by using a collimator implemented with a Grin lens, and the interference signal produced by reflection on both sides of the plate was directed through the Bragg gratings[25–27] and, after that, toward the detection system. As stated above (Sec. 3, Fig. 6), the calibration curve of the implemented system is linear, then only two FBGs were used to determine the sampling rate.

FBGs used were centered at 1526.28 nm (FBG_1) and 1539.31 nm (FBG_2), with 3 dB spectral widths of 0.20 and 0.12 nm, and reflectivities of 52.3% and 99.6%, respectively. They were characterized by using an optical sensor interrogation module (Micron Optics, model sm125) and an OSA.

The input signal to the FP filter was configured with a voltage of 20 Vpp and 20 ms period, as shown in Fig. 10 (a). The interference signal is shown in Fig. 10(b). The temporary location of the Bragg gratings can also be observed. This temporal distribution was obtained employing a Teledyne LeCroy WaveRunner 610Zi digital oscilloscope and the internal photodetector of the FFP-C.

By performing the Fourier transform of the interference signal and employing the calibration process described before, the thickness value measured was 1.14 mm (Fig. 11). In this case, we used a tuning range of 60 nm; the axial resolution was ~40 μm.

In order to verify this measurement, we employed an OSA (Yokogawa, model AQ6370B) with 0.02-nm resolution. As the OSA has a large acquisition time compared to the minimum frequency of the laser scanning, we used as an alternative broadband source the amplified spontaneous emission (ASE) of an erbium-doped fiber amplifier.

The recorded signal obtained with the OSA is shown in Fig. 12, where it can be distinguished the attenuation peaks generated by the Bragg filters (at 1526.28 and 1539.31 nm), and the laser emission at an arbitrary wavelength within the tuning range, over the ASE spectral distribution.

In this case the peak of the Fourier transform is at 1.13 mm, as shown in Fig. 13, being practically coincident with the temporal measurement corresponding to Fig. 10.

Comparing this result with that obtained by the proposed system, we see that the difference is 0.7%, compatible with the value mentioned in Sec. 3.

4.2 *Measurement of Large Distances*

To apply the proposed system to measure distances over 1 cm, a Michelson interferometer similar to that shown in Fig. 4 was mounted. The illumination beam was divided

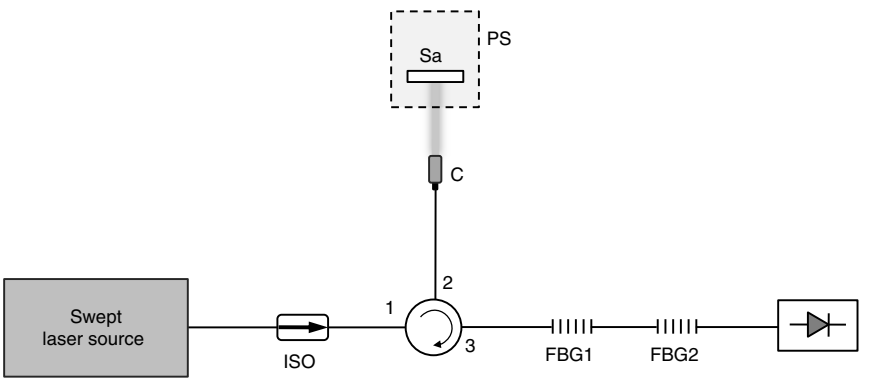

Fig. 9 Experimental configuration for thickness measurements.

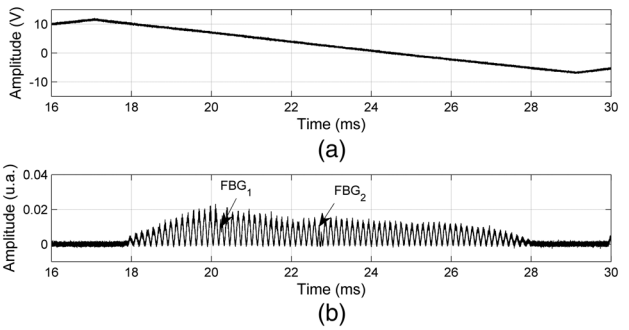

Fig. 10 (a) PZT excitation signal and (b) interference signal.

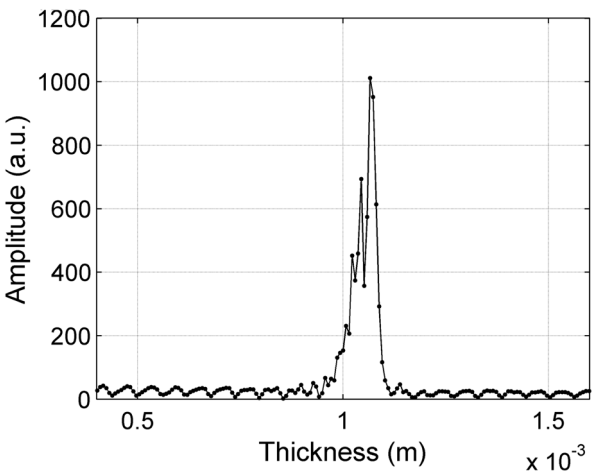

Fig. 11 Interference peak.

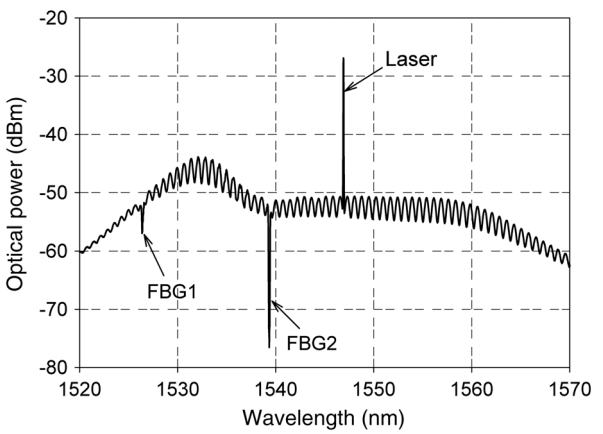

Fig. 12 ASE spectrum showing the attenuation peaks generated by the Bragg filters.

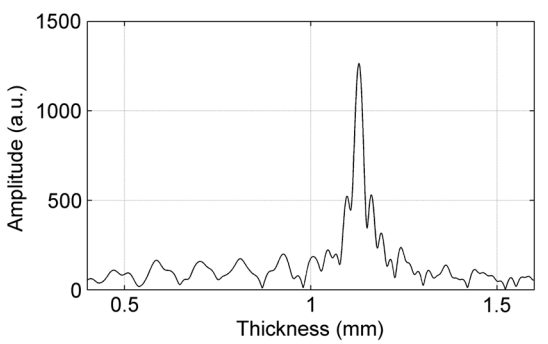

Fig. 13 Fourier transform indicating the thickness.

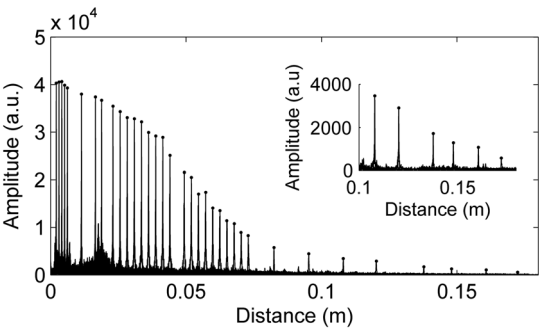

Fig. 14 Normalized amplitude of the Fourier peaks corresponding to different OPDs.

by a 2×1, 50/50 single mode fiber coupler and the outputs were collimated to impinge on the sample (mirror M1) and on the reference (mirror M2).

With the aim of searching the limit in measuring depth of the system, a device was designed where it was possible to place the sample mirror in preset positions separated 5 cm, while the reference was mounted on a translation stage with a micrometer drive of 5-cm travel. By combining the displacements of both mirrors, a continuous variation of the distance to be measured was obtained.

The interference signals were processed by using the Hilbert–Fourier transform and the corresponding results are plotted in Fig. 14. A wide range of OPD values was covered, reaching up to 17.24 cm.

Mainly due to the divergence of the collimator and the coherence length of the light source, the amplitude of the interference peaks was attenuated as the OPD was increased. This drop in the visibility of the processed signal can be seen in Fig. 14. The lower the scanning speed, the higher the coherence length, which decreased the effect of attenuation. For the implemented system, the depth of measurement or maximum achievable measurement range was limited to about 17 cm.

5 Conclusions

This paper has presented and experimentally demonstrated a coherent optical tomography system that offers the possibility of measuring distances up to 17 cm using a tunable light source in the spectral region of 1550 nm, which uses an FP filter driven by a piezoelectric actuator. This scheme is complemented by a passive self-calibration system consisting of an array of FBGs, which can be used superimposed on the signal to be measured or in a separate channel. With this system, it is possible to monitor the spectral position of the light source in each scan and correct errors due to nonlinearity of the piezoelectric actuator or the repetition cycle control. From the results obtained by characterizing the system, it has been observed that if the gratings suffer thermal variations, it is imperative that all of them experience the same temperature change, because in this way they will move equally in wavelength without affecting the calibration scheme. In this way, temperature changes have no influence on the system.

It should be noted that the objective of the work performed was to obtain the greatest possible measurement range rather than optimizing the axial resolution, which

depends on the spectral shape and scan width of the light source used.

We believe that with schemes similar to the proposed ones, progress can be made in little explored applications of reflectometry, such as in the determination of dimensional parameters of mechanical parts, and tomography for the study of transparent and semitransparent materials (glass, plastics, polymers, etc.) of large dimensions.

Acknowledgments

This work has been supported by the Consejo Nacional de Investigaciones Científicas y Tecnológicas CONICET (PIP 112-201101-00397); Facultad de Ingeniería-Universidad Nacional de la Plata (Project I169), Comisión de Investigaciones Científicas de la Pcia. de Buenos Aires CIC (Resolución No 243/13), and Facultad Regional Delta, UTN, PID 2221, Campana, Argentina.

References

1. D. Huang et al., "Optical coherence tomography," *Science* **254**, 1178–1181 (1991).
2. A. F. Fercher et al., "Measurement of intraocular distances by backscattering spectral interferometry," *Opt. Commun.* **117**, 43–48 (1995).
3. F. Lexer et al., "Wavelength-tuning interferometry of intraocular distances," *Appl. Opt.* **36**, 6548–6553 (1997).
4. G. Häusler and M. W. Lindner, "'Coherence radar' and 'spectral radar'-new tools for dermatological diagnosis," *J. Biomed. Opt.* **3**, 21–31 (1998).
5. S. A. Boppart et al., "Noninvasive assessment of the developing Xenopus cardiovascular system using optical coherence tomography," *Proc. Natl. Acad. Sci. U. S. A.* **94**, 4256–4261 (1997).
6. J. Rogowska, C. M. Bryant, and M. E. Brezinski, "Cartilage thickness measurements from optical coherence tomography," *J. Opt. Soc. Am. A* **20**, 357–367 (2003).
7. R. Leitgeb, C. K. Hitzenberger, and A. F. Fercher, "Performance of Fourier domain vs. time domain optical coherence tomography," *Opt. Express* **11**, 889–894 (2003).
8. R. Chinn, E. A. Swanson, and J. G. Fujimoto, "Optical coherence tomography using a frequency-tunable optical source," *Opt. Lett.* **22**, 340–342 (1997).
9. Insight, Akinetic All-Semiconductor Technology, http://www.sweptlaser.com/high-speed-sweeping (2016).
10. Thorlabs, MEMS-VCSEL Swept Source OCT, http://www.thorlabs.com/newgrouppage9.cfm?objectgroup_id=6473 (2016).
11. R. Huber et al., "Amplified, frequency swept lasers for frequency domain reflectometry and OCT imaging: design and scaling principles," *Opt. Express* **13**, 3513–3528 (2005).
12. M. Bonesi et al., "Akinetic all-semiconductor programmable swept-source at 1550 nm and 1310 nm with centimeters coherence length," *Opt. Express* **22**, 2632–2655 (2014).
13. R. Huber, M. Wojtkowski, and J. G. Fujimoto, "Fourier domain mode locking (FDML): a new laser operating regime and applications for optical coherence tomography," *Opt. Express* **14**, 3225–3237 (2006).
14. R. Huber, D. C. Adler, and J. G. Fujimoto, "Buffered Fourier domain mode locking: unidirectional swept laser sources for optical coherence tomography imaging at 370,000 lines/s," *Opt. Lett.* **31**, 2975–2977 (2006).
15. D. C. Adler, R. Huber, and J. G. Fujimoto, "Phase-sensitive optical coherence tomography at up to 370,000 lines per second using buffered Fourier domain mode-locked lasers," *Opt. Lett.* **32**, 626–628 (2007).
16. S. W. Huang et al., "Swept source optical coherence microscopy using a Fourier domain mode-locked laser," *Opt. Express* **15**, 6210–6217 (2007).
17. R. Huber et al., "Fourier domain mode locking at 1050 nm for ultra-high-speed optical coherence tomography of the human retina at 236,000 axial scans per second," *Opt. Lett.* **32**, 2049–2051 (2007).
18. K. Iiyama, L. T. Wang, and K. I. Hayashi, "Linearizing optical frequency sweep of a laser diode for FMCW reflectometry," *J. Lightwave Technol.* **14**, 173–178 (1996).
19. I. Grulkowski et al., "High-precision, high-accuracy ultralong range swept-source optical coherence tomography using vertical cavity surface emitting laser light source," *Opt. Lett.* **38**, 673–675 (2013).
20. C. M. Eigenwillig et al., "K-space linear Fourier domain mode locked laser and applications for optical coherence tomography," *Opt. Express* **16**, 8916–8937 (2008).
21. A. Bradu, L. Neagu, and A. Podoleanu, "Extra long imaging range swept source optical coherence tomography using re-circulation loops," *Opt. Express* **18**, 25361–25370 (2010).
22. R. Kashyap, *Fiber Bragg Gratings*, 2nd ed., Academic Press, Elsevier, San Diego (2009).
23. A. Othonos and K. Kalli, *Fiber Bragg Gratings: Fundamentals and Applications in Telecommunications and Sensing*, Artech House, Boston (1999).
24. T. J. Eom et al., "Calibration and characterization protocol for spectral-domain optical coherence tomography using fiber Bragg gratings," *J. Biomed. Opt.* **16**(3), 030501 (2011).
25. S. H. Yun, D. J. Richardson, and B. Y. Kim, "Interrogation of fiber grating sensor arrays with a wavelength-swept fiber laser," *Opt. Lett.* **23**, 843–845 (1998).
26. A. Giordana and R. Duchowicz, "Development and analysis of a simple tunable erbium ring laser," *Proc. SPIE* **8011**, 80115A (2011).
27. S. Yamashita and M. Nishihara, "Widely tunable erbium-doped fiber ring laser covering both C-band and L-band," *IEEE J. Sel. Top. Quantum Electron.* **7**, 41–43 (2001).
28. H. Chen et al., "Widely tunable single-frequency erbium-doped fiber lasers," *IEEE Photonics Technol. Lett.* **15**, 185–187 (2003).
29. S. K. Liaw, K. C. Hsu, and N. K. Chen, "Tunable erbium-doped fiber lasers using various inline fiber filters," *Engineering* **2**, 585–593 (2010).
30. Y. Shen et al., "Extended range phase-sensitive swept source interferometer for real-time dimensional metrology," *Opt. Commun.* **318**, 88–94 (2014).
31. A. V. Oppenheim and R. W. Schafer, *Discrete-Time Signal Processing*, 2nd ed., Prentice-Hall (1998).
32. J. Na et al., "Image restoration method based on Hilbert transform for full-field optical coherence tomography," *Appl. Opt.* **47**, 459–466 (2008).
33. L. R. Rabiner and B. Gold, *Theory and Application of Digital Signal Processing*, Prentice-Hall, Englewood Cliffs, New Jersey (1975).

Eneas N. Morel is an electronic engineer and graduated from Faculty of Engineering of UNLP. He received his PhD degree from Delta Regional Faculty of the National University of Technology in 2010. He is currently a researcher at the Laboratorio de Optoelectrónica y Metrología Aplicada, Facultad Regional Delta, UTN and a member of CONICET. His research focuses mainly on low-coherence interferometry applied to general metrology and optical coherence tomography applied to the study of materials.

Nélida A. Russo is a researcher at the Commission of Scientific Research of Buenos Aires Province (CIC), Argentina. She received her PhD and MS degrees in engineering from UNLP, Argentina, in 1985 and 2006, respectively. She worked as an assistant professor of physics at the Faculty of Engineering of UNLP. In 1988, she joined the Optical Research Center (CIOp), Argentina, and her current research interests include optical fiber applications in sensors, lasers, and optical communications.

Jorge R. Torga received his degree in physics and the PhD degree in sciences from University of Buenos Aires in 1992 and 1997, respectively. He is currently a researcher at the Laboratorio de Optoelectrónica y Metrología Aplicada, Facultad Regional Delta, National University of Technology and a researcher at CONICET, Argentina. His research focuses mainly on optical coherence tomography and low-coherence interferometry techniques.

Ricardo Duchowicz is a researcher of the CONICET and professor from the Faculty of Engineering of UNLP, Argentina. He received his PhD and MS degrees in physics from UNLP in 1981 and 1977, respectively. In 1977, he joined the CIOp. He has published extensively on subjects related to fiber optic lasers, fiber sensors, and pulse transmission in fiber optic links.